# Microstructure and mechanical properties of plasma sprayed $Al_2O_3$ – 13%$TiO_2$ Ceramic Coating

Juyana A Wahab[1,2], Mariyam Jameelah Ghazali[1,a] and Ahmad Firdaus Shamsul Baharin[1]

[1]*Department of Mechanical & Materials Engineering, Faculty of Engineering and Built Environment, Universiti Kebangsaan Malaysia, 43600 UKM Bangi, Selangor, Malaysia*
[2]*School of Materials Engineering, Universiti Malaysia Perlis, Kompleks Pusat Pengajian Jejawi 2, Taman Muhibah, 02600 Jejawi, Arau, Perlis, Malaysia.*

**Abstract.** This paper focused on the effect of deposition conditions on the microstructural and mechanical properties of the ceramic coating. In this study, $Al_2O_3$ – 13%$TiO_2$ coated mild steel were prepared by using atmospheric plasma spray technology with different plasma power ranging from 25 kW to 40 kW. The as-sprayed coatings consist of γ-Al2O3 phase as the major phase and small amount of the titania phase existed in the coating structure. High degree of fully melted region was observed in the surface morphology for the coating sprayed with high plasma power, which lead to the high hardness and low percentage of porosity. In this study, nanoindentation test was carried out to investigate mechanical properties of the coating and the results showed that the coatings possess high elastic behaviour, which beneficial in engineering practice.

## 1 Introduction

The research and manufacturing of ceramic coatings had gained great attention due to their excellent characteristics and potential applications. Most of ceramic material presenting useful features such as low density, excellent wear resistance, high inertness, high stability and high temperature strength [1, 2]. These features resulted by high atomic strength of ceramic that led to its great hardness, strength and stiffness. Ceramics also possess high resistance to oxidation as well as corrosion in extreme condition and thus make them having a wide range of applications especially in structural and engineering fields [3].

Development of new materials has affected ceramic film and coating technology. The relatively high hardness and inertness of ceramic coating led to its excellent performance as a protective layer on substrate surface in order to mitigate corrosion, oxidation and wear problem especially in marine environment. Oil and gas industry, shipping industry and the marine structures suffer from corrosion due to the exposure of aggressive ions in seawater. Combinations of wear, oxidation and corrosion problems contribute to failure factors that would eventually cause total shutdown, economic loss and hazardous effects [4]. For these reasons, applying coating protection method to material surface is very important. Various types of ceramic coating gained attention to overcome these problems such as alumina ($Al_2O_3$), titanium carbide (TiC), silicon nitride ($Si_3N_4$) [5], titanium nitride ($TiNiO_3$) [6], alumina-titania ($Al_2O_3$-$TiO_2$) [7-10], alumina-titania-zirconia ($Al_2O_3$-$TiO_2$-$ZrO_2$) [11], chromium oxide ($Cr_2O_3$-Ag) [12] and titanium diborate ($TiB_2$). Such ceramic coatings can be produced using thermal spraying technology, CVD, PVD and sputtering. Previous studies stated that among these techniques, atmospheric plasma spraying technique is an effective technique for deposition of thick coating on the substrates [13]. It is the most commonly used thermal spraying technology due to its high flexibility, high deposition consistency and high deposition rates. It is known that the condition and properties of plasma sprayed coating is strictly influenced by plasma spraying process parameters, which are stand-off distance, plasma power and gas pressure. These parameters directly affect the heat and mass transfer between powder particles and plasma and thus influence the degree of powder particles melting and the structure of droplets on the coating surface [14].

The mechanical properties and the surface morphology of the coating are affected by the spraying conditions that are plasma spray power, stand-off distance and powder feeding rate. These parameters affect the thermal and kinetic energy of the powder particles. If the powder particles gained an extra thermal energy, the vapourisation of the powder particles take place in the plasma jet before impact onto the substrate surface in the fully-melted condition [15]. However, if the powder particles gained small amount of thermal energy, they will reach onto the substrate surface in a partially-melted condition. Both of these two condition will affect the characteristics of the coating. Venkataraman et al. [16] investigated the effect of porosity, pore size and pores distribution on the hardness

[a] Corresponding author: mariyam@ukm.edu.my

of plasma sprayed ceramic coatings. They claimed that among several microstructural features, porosity generated by partially melted particles has a major effect on the hardness of the coating.

In this work, nanoindentation is utilised in order to measure mechanical properties of materials. It has recently begun to be utilized widely in thermally sprayed materials but the results are always complicated to analyse. This technique measures the coating hardness as well as elastic modulus by considering the degree of the material deformation. The deformation mechanisms upon mechanical loading during the test always considered as properties that depends on the testing conditions. Therefore, in this study, the nanoindentation technology was utilized to determine the effect of indentation load and depth of the measured mechanical properties of thermally sprayed $Al_2O_3$ - 13%$TiO_2$ coating.

## 2 Materials and method

### 2.1 Plasma spraying

Mild steel (ASTM A36) was used in this study as substrate material with dimension of 25 x 10 x 3 mm. The commercial feedstock $Al_2O_3$ – 13%$TiO_2$ (Metco 130SF) was mechanically clad having a fine particle distribution (–45+5 µm) was deposited vertically onto the substrates by atmospheric plasma spraying (APS) using a plasma torch (Praxair SG-100) mounted on a programmable robot. The surface of the substrates was grit-blasted with $Al_2O_3$ before coating to increase the roughness and the mechanical interlocking between coating and substrate. The thickness of coating was fixed to be within 200–300 µm. The deposition parameters set for the spraying process are shown in Table 1.

**Table 1.** Plasma spraying parameter.

| Parameter | Value |
|---|---|
| Plasma power (kW) | 25 – 40 |
| Primary gas pressure (Psi) | 80 |
| Secondary gas pressure (Psi) | 60 |
| Carrier gas pressure (Psi) | 40 |
| Powder feed rate (Rpm) | 3 |
| Coating speed (mm/s) | 250 |
| Stand-off distance (mm) | 100 |

### 2.2 Characterisation and testing

For the characterisation techniques, all metallography samples were ground and polished to obtain mirror-like surface finish. The morphology of feedstock and as-sprayed coating was observed under a LEO 1430 VP scanning electron microscope (VPSEM). The phase composition existed in the powder feedstocks and the coatings was examined using an X-Ray powder diffractometer (XRD) model Bruker, D8- Advance 2009, Germany with CuKα (λ=0.1541 nm) radiation source. A software of image analysis was used to calculate the coating porosity. The quote values are an average of 10 areas of coating cross-section images observed at 1000× magnification. The porosity of coating was calculated based on the standard of ASTM E2109-01. A HMV-2 T Vickers microhardness tester was used to measure the microhardness of the coating. 25 readings were taken at different dense locations with the 300 g applied load and the dwell time was set to 15 s. For measurement of nanomechanical properties, the indentations were performed on polished cross section of coating samples using Micro Materials Nanotest$^{TM}$ indenter equipped with a Berkovich diamond tip. Ten indentations were made on each sample. The indentation load was set at 50mN and the maximum load was held constant for 5s. The loading rate was applied at 1mN/s.

## 3 Results and discussion

### 3.1 Phase composition and microstructure

Five levels of plasma spray power were applied to examine the characteristic of microstructure and nanoindentation behaviour of the coating. As shown in Figure 1, alumina-titania powder is consisted of α-$Al_2O_3$ phase, while the as-sprayed coating is consisted of γ-$Al_2O_3$ phase (major) and α-$Al_2O_3$ (minor). This result showed that the powders have experienced a phase transformation from α phase to γ phase during the deposition process. This transformation was due to a rapid cooling effect. Some amount of titania phases in the form of aluminium titanate ($Al_3Ti_5O_2$) were also identified. However, the amount of $Al_2TiO$ phase was very low due to the reaction of alumina as titania was dissolved into γ-$Al_2O_3$ during the deposition process [17].

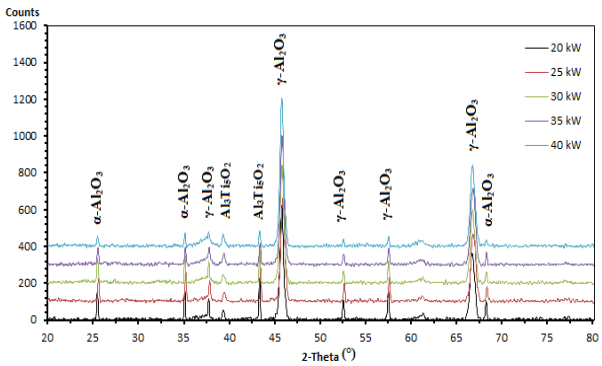


**Figure 1.** XRD pattern of as-sprayed $Al_2O_3$ -13%$TiO_2$ coating

Figure 2 shows the SEM micrographs of as-sprayed coating at four different plasma powers. It can be seen that high amount of unmelted particles with larger size was retained within the surface at low plasma power coating. The deposition exhibited uniform and large sized droplets with less porosity at high plasma power coating. At high plasma power, it was clearly noted that there was larger fully melted region of powder particles resulting thinner and better contact between splats of the coating surface.

The cross sectional of the coatings is shown in the Figure 3. It was revealed that higher plasma power resulted in less porosity within the coating. High plasma

power generated higher temperature thus resulting an increase in the fully melted region on the coating structure [18]. This factor contributed to the denser coating structure with low percentage of porosity. Figure 4 illustrates the average percentage of porosity formed in the coating. The average percentage of porosity in the coating gradually decreased as the plasma power increased.

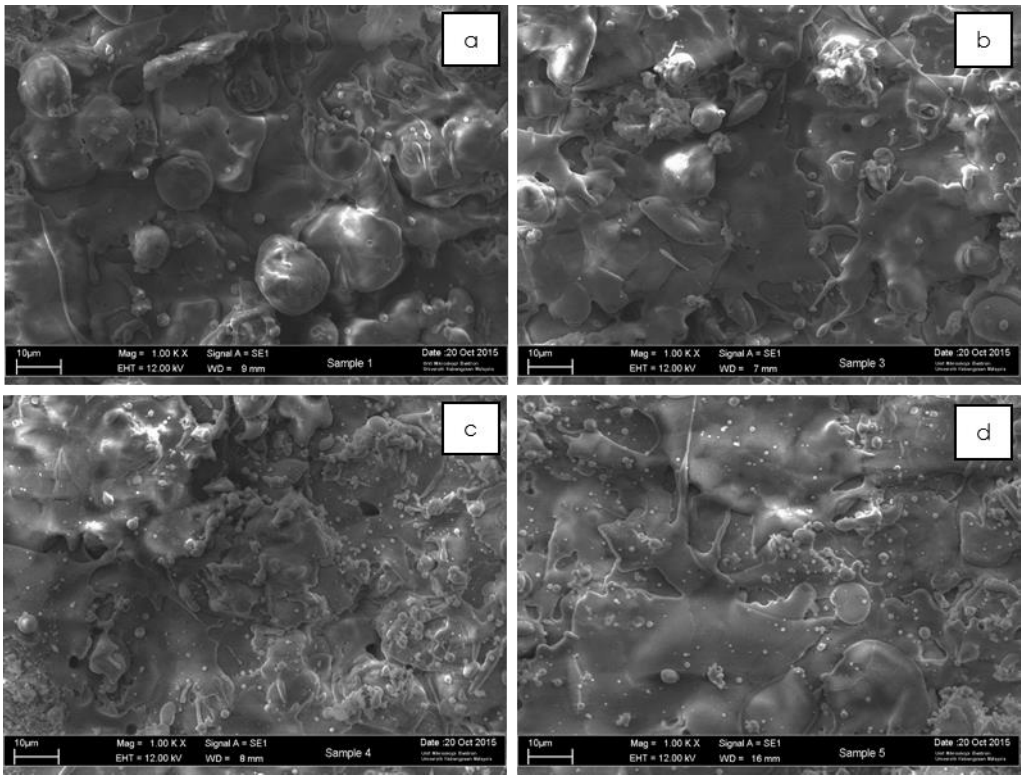


**Figure 2.** Surface morphology of $Al_2O_3$ -13%$TiO_2$ coating a) 25 kW, b) 30 kW, c) 35 kW and d) 40 kW of plasma power.

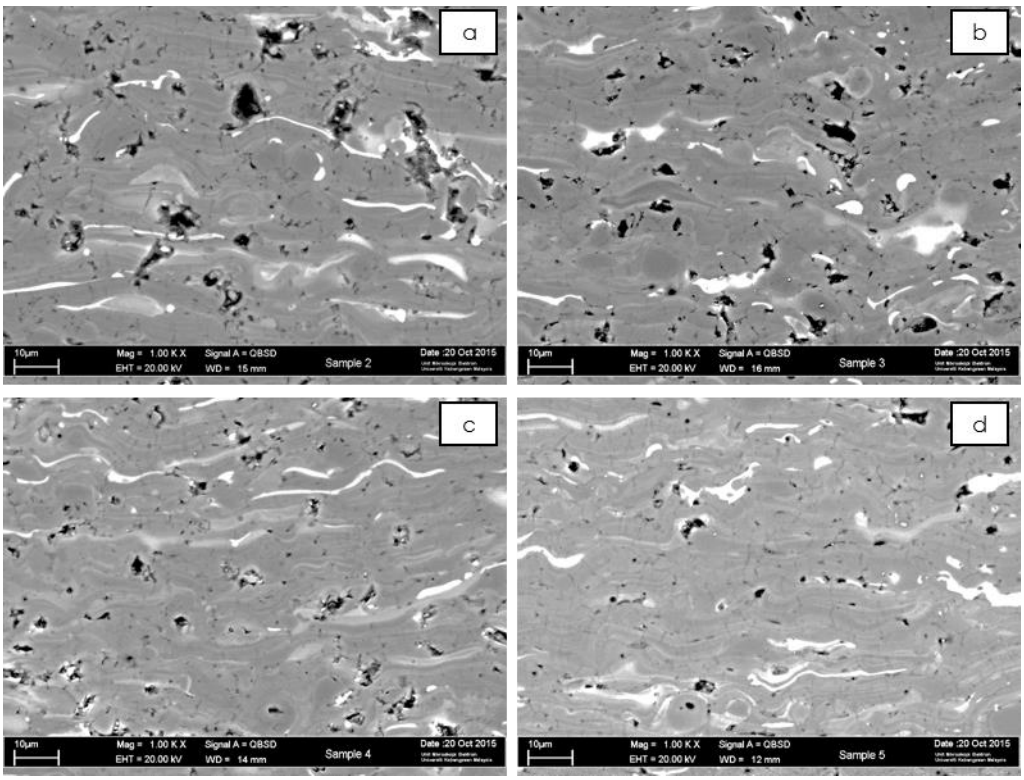


**Figure 3.** Cross sectional of $Al_2O_3$ -13%$TiO_2$ coating a) 25 kW, b) 30 kW, c) 35 kW and d) 40 kW of plasma power.

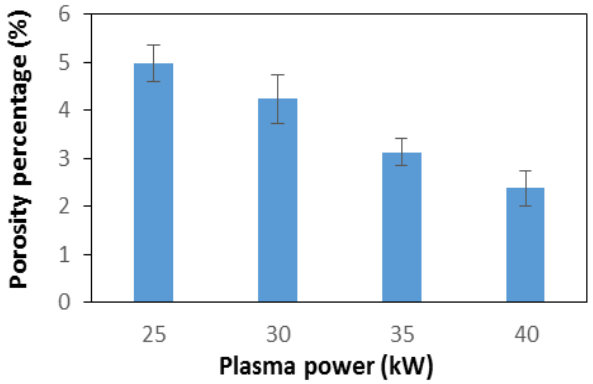


**Figure 4.** Percentage of porosity of plasma sprayed $Al_2O_3$ - 13%$TiO_2$ coating

### 3.2. Nanoindentation

As stated in earlier sections, plasma power is one of the key factors that affect the microstructure of plasma sprayed ceramic coating. Generally, high plasma power induced high current that led to the high deposition temperature. This would increase the melting fraction of powder particles and reduced the porosity. According to Yusoff, et al. [19], porosity in the coating affected the mechanical properties of the coating particularly, the hardness properties. Figure 5 presents the hardness of the coating. It was noted that a slight increase had occurred as the plasma power was raised up to 40 kW. Thus, this indicates that high percentage of coating porosity contributed to a lower hardness of the coating.

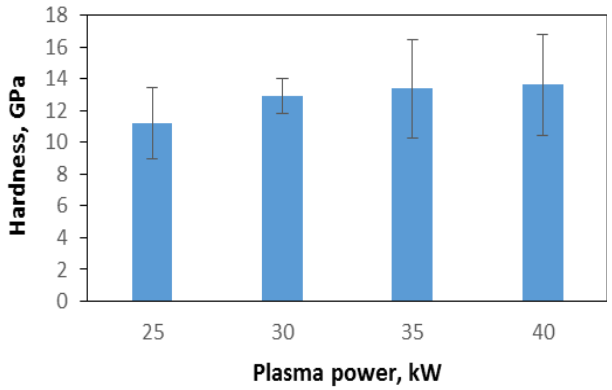


**Figure 5.** Hardness of plasma sprayed $Al_2O_3$ -13%$TiO_2$ coating

Figure 6 shows the loads as a function of indentation depths of the coating. Differences in hardness of the coating were indicated by the depth attained at the maximum load. It was found that at 50 mN load, the penetration depth for 25 kW plasma power coating was far greater than 500 nm, compared to the higher plasma power coating which were only around 450 nm. Other than that, the ceramic coatings show high degree of elastic recovery during unloading which contributed to the low plastic deformation during the indentation process. Large elastic recovery in coatings is beneficial in reducing the damage by impact and abrasive wear.

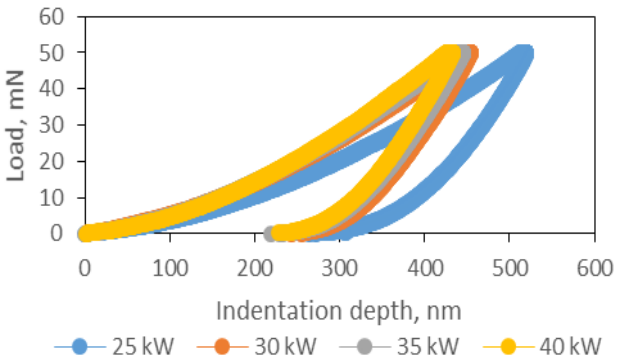


**Figure 6.** Load-displacement curve of plasma sprayed $Al_2O_3$ - 13%$TiO_2$ coating

In the previous section, it was clearly noted that the spraying power directly affect the heat and mass transfer between powder particles and plasma and then influence the degree of powder particles melting and the structure of droplets on the coating surface. High plasma power resulted in denser coating with low porosity. It occurs when high current induced by high plasma power generates high energy to facilitate more ionization of the gases flowing between the electrodes to form plasma plume. As the temperature of the plasma plume increase, a tremendous level of thermal energy is released so that the feedstock material has sufficient energy to melt completely when injected into hot plasma plume and then propelled towards the target substrate to form the denser coating.

## 4 Conclusion

$Al_2O_3$ -13%$TiO_2$ coatings were deposited onto mild steel using atmospheric plasma spray technology by varying the plasma power from 25 kW to 40 kW. The microstructure and mechanical properties of the coatings varied with the applied plasma power. It can be concluded that high temperatures resulted a high melting degree of the powder particles deposition that led to a denser coating structure with lower percentage of porosity. From the nanoindentation test, the high plasma power at 40 kW resulted the highest hardness of coating; 13.63 GPa, whereas at 25 kW, little hardness of coating about 11.21 GPa, was recorded. In short, all coatings showed good elastic properties, which are beneficial in most of engineering applications.

## Acknowledgement

This work was financially supported by the Universiti Kebangsaan Malaysia grant number (DIP-2014-003). The author also acknowledges the Universiti Malaysia Perlis, UniMAP and Ministry of Education Malaysia (KPM) and for their meaningful supports and co-operations.

## References

1. Y. Xing, J. Deng, X. Feng, and S. Yu, Materials & Design, **52**, 234-245 (2013)
2. A. N. Samant and N. B. Dahotre, Journal of the European Ceramic Society, **29**, 969-993 (2009)
3. J. B. Wachtman and R. A. Haber, *Ceramic Films and Coatings* (United States, Noyes Publications, 1993)
4. M. A. Zavareh, A. A. D. M. Sarhan, B. B. A. Razak, and W. J. Basirun, Ceramics International, **40**, 14267-14277 (2014)
5. Y. Xing, J. Deng, Z. Wu, and H. Cheng, Applied Surface Science, **265**, 823-832 (2013)
6. Y. Xing, J. Deng, Y. Zhou, and S. Li, Surface and Coatings Technology, **258**, 699-710 (2014)
7. Y. Yang, Y. Wang, W. Tian, D.-r. Yan, J.-x. Zhang, and L. Wang, Materials & Design, **65**, 814-822 (2015)
8. E. Bannier, M. Vicent, E. Rayón, R. Benavente, M. D. Salvador, and E. Sánchez, Applied Surface Science, 316, 141-146 (2014)
9. W. Tian, Y. Wang, and Y. Yang, Tribology International, **43**, 876-881, (2010)
10. E. P. Song, J. Ahn, S. Lee, and N. J. Kim, Surface and Coatings Technology, **202**, 3625-3632 (2008)
11. Y. Yang, D. Yan, Y. Dong, X. Chen, L. Wang, Z. Chu, Vacuum, **96**, 39-45 (2013)
12. E. Sadri and F. Ashrafizadeh, Surface and Coatings Technology, **236**, 91-101 (2013)
13. G. Di Girolamo, A. Brentari, C. Blasi, and E. Serra, Ceramics International, **40**, 12861-12867 (2014)
14. D. Thirumalaikumarasamy, K. S. Kamalamoorthy, and V. B. Visvalingam, Journal of Magnesium and Alloys, **3**, 237-246 (2015)
15. Wang, H.-d. Ma, J.-l. Li, G.-l. Kang, J.-j. and. Xu, B.-s , Applied Surface Science, **314**, 468-475 (2014)
16. R. Venkataraman, G. Das, S. R. Singh, L. C. Pathak, R. N. Ghosh, B. Venkataraman, Materials Science and Engineering: A, **445–446**, 269-274 (2007)
17. D. Goberman, Y. H. Sohn, Shaw, Jordan, and M. Gell, Acta Materialia, **50,** 1141–1152 (2000)
18. M. J. Ghazali, S. M. Forghani, N. Hassanuddin, Muchtar, and A. R. Daud, Tribology International, **93,** 681-686 (2016)
19. N. H. N. Yusoff, M. J. Ghazali, M. C. Isa, A. R. Daud, A. Muchtar, and S. M. Forghani, Materials & Design. 39: 504-508 (2012)